Micromachining of Crosslinked PTFE by Direct Photo-Etching Using Synchrotron Radiation

Daichi Yamaguchi[1]*, *Takanori Katoh*[2], *Yasunori Sato*[1], *Shigetoshi Ikeda*[3], *Masaoki Hirose*[2], *Yasushi Aoki*[2], *Minoru Iida*[3], *Akihiro Oshima*[1], *Yoneho Tabata*[4], *Masakazu Washio*[1]

[1]Advanced Research Institute for Science and Engineering, Waseda University, 3-4-1, Okubo, Shinjuku-ku, Tokyo, 169-8555 Japan
[2]Sumitomo Heavy Industries, Ltd., 2-1-1, Yato-cho, Nishitokyo, Tokyo, 188-8585 Japan
[3]Raytech Corporation, #402 Sousyu Bldg., 4-40-13, Takadanobaba, Shinjuku-ku, Tokyo, 169-0075 Japan
[4]Professor Emeritus, The University of Tokyo, 7-3-1, Hongo, Bunkyo-ku, Tokyo, 113-8656 Japan

Summary: Micromachining of crosslinked PTFE (polytetrafluoroethylene) using synchrotron radiation direct photo-etching method has been demonstrated. High aspect-ratio microfabrication was carried out. The etching rate of crosslinked PTFE was higher than that of non-crosslinked PTFE. Through the etching rate measurements of various samples, it was found that synchrotron radiation etching rate of crosslinked PTFE only depends on the degree of crosslinking, neither molecular weight nor crystallinity. The effect of molecular motion on etching process was discussed from temperature dependence data on etching rate. Furthermore, the surface region of synchrotron radiation irradiated sample was investigated by Fourier transform infrared spectroscopy and the experimental result showed that the modification induced by synchrotron radiation proceeded before desorption.

Introduction

Polytetrafluoroethylene (PTFE) is a very unique polymeric material because of the various distinguished properties such as high electrical resistivity, chemical and thermal stability, potential biocompatibility and so on.[1] These advantageous features enable PTFE to be applied in a variety of areas including electronics and medical field. However, PTFE is used less in nuclear facilities or aerospace environment, since PTFE is very sensitive to ionizing radiation.[1,2] PTFE is degraded by radiation with a low dose through main chain scission and mechanical properties are seriously deteriorated extremely. Recently, crosslinked PTFE was found to be obtained by ionizing radiation around the melting temperature under oxygen free atmosphere.[3-7] It was reported that elevating irradiation temperature promotes the chain mobility and greatly enhances recombination of radicals induced by ionizing radiation. Radiation crosslinking reaction

 CCC 1022-1360/00/$ 17.50+.50/0

of PTFE causes the various changes of properties. The radiation durability and mechanical properties are much improved by crosslinking.[5,7,8] While the color of non-crosslinked PTFE is white, crosslinked PTFE is transparent due to a decrease in crystallinity. Detail studies on the chemical structure of high-resolution solid state ^{19}F and ^{13}C high-speed MAS NMR spectroscopy showed that the structure of the crosslinking point should be of a Y-type structure formed by combination reaction between chain end radical and chain alkyl radical, whereas an H-type structure is preferably formed by recombination reaction among chain alkyl radicals.[9,10]

Crosslinked PTFE has the potential to be applied as a microcomponent on the basis of the properties mentioned above. Several reports concerning microfabrication of non-crosslinked PTFE have been published so far. Pulsed laser ablation technique using vacuum ultraviolet (VUV) laser[11] or ultrashort pulsed laser[12] have been attempted to create microstructures of PTFE. However, the aspect-ratio, which is the ratio of the depth of the microstructures to the pattern width, was up to 1. So, laser ablation technique should not be appropriate to create high aspect-ratio microstructures of PTFE. On the other hand, it was reported that synchrotron radiation (SR) is a powerful tool for micromachining of non-crosslinked PTFE.[13,14] Non-crosslinked PTFE is efficiently decomposed by SR and a desorption of fragments induced by SR irradiation occurs consequently. Since this method requires no additional chemicals to produce microstructures, this fabrication technique is simpler and can be performed in shorter time than any other fabrication methods. The maximum aspect-ratio of over 50 was achieved using this technique.

The preliminary results of microfabrication for crosslinked PTFE using SR were reported in our previous paper.[15] It was found that crosslinked PTFE could also be etched, the etching rate of crosslinked PTFE being higher than the one of non-crosslinked PTFE. In this paper, we describe recent studies on micromachining of crosslinked PTFE and SR etching mechanism for both, PTFE and crosslinked PTFE.

Experimental

Materials

PTFE sheets with a thickness of 0.5 mm were obtained from Asahi Grass Fluoropolymers Co. Ltd. Two other types of non-crosslinked PTFE samples, low crystallinity sample (LC) and low molecular weight sample (LM), were also prepared. LC was obtained by quenching from the molten state and LM was obtained by ^{60}Co γ-

irradiation with a dose of 10 kGy at room temperature under vacuum condition. Crosslinked PTFE samples (RX) were prepared by electron beam (EB) irradiation in its molten state at 613 K in argon atmosphere (0.5 $kGy \cdot s^{-1}$).[5] Other crosslinked PTFE samples, LMRX-1600, were made from LM by EB irradiation of 1600 kGy in the molten state. The basic data of the samples prepared for this work are summarized in Table 1.

Table 1. Data of samples prepared. Cryatallinity was determined by X-ray diffraction[16] and molecular weigtht was determined by differential scanning calorimeter (DSC) in method.[17]

Sample name	Dose for crossilnking [kGy]	Crystallinity [%]	Molecular weight
native PTFE	0	76.1	9.8×10^6
LC	0	58.9	9.8×10^6
LM	0	93.3	$< 1.0 \times 10^5$
RX-1600	1600	49.3	-
RX-3000	3000	15.9	-
LMRX-1600	1600	51.1	-

Microfabrication by SR direct photo-etching

The experiments were performed using SR microfabrication beamline (BL-4) of the compact normalconducting electron storage ring, AURORA-2S (manufactured by Sumitomo Heavy Industries, Ltd.).[18] BL-4 delivers wide spectrum range light covering the energy range from IR to X-ray region. The photon energy spectrum of AURORA-2S is shown in Figure 1. The samples were placed perpendicular to the SR beam in the vacuum chamber and were irradiated by the SR beam through a beryllium (Be) filter with a thickness of 10 μm in order to cut off longer wavelengths deforming the transferred pattern due to local heating of sample. The photon flux of the SR beam through the Be-filter was 3.2×10^{11} $photons \cdot s^{-1} \cdot mA^{-1} \cdot mm^{-2}$. A Ni mesh was set on the sample to transfer the pattern. The proximity X-ray mask was also used in some cases (Figure 2). The temperature of the samples was controlled from room temperature to 473 K by a hot plate which was placed behind the samples.

Measurements

The microstructures created by SR direct photo-etching were observed by scanning electron microscopy (SEM) and the etching depth was measured by optical microscope. The surfaces of the samples were analyzed by Fourier transform infrared spectroscopy

(FT-IR; JES-6000 provided by JEOL) for the investigation of the SR etching mechanism.

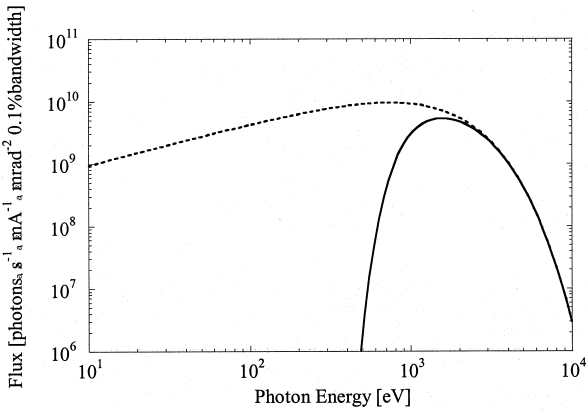

Figure 1. Energy spectra of AURORA-2S; SR: dotted line, filtered SR (Be 10 μm): solid line.

Results and discussion

Etching rate measurements

Microfabrication of crosslinked PTFE by SR photo-etching was carried out successfully. The SEM photograph of microstructure of RX-1600, which was created by the irradiation at 413 K, is shown in Figure 2. It was confirmed that the quality of micromachining of crosslinked PTFE is as good as that of non-crosslinked PTFE.[15]

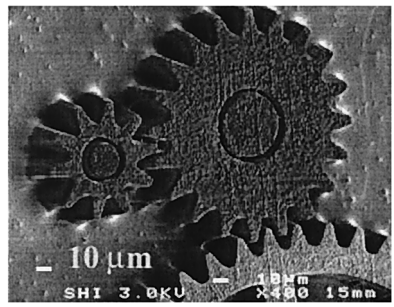

Figure 2. Micro-gear made of RX-1600 by SR direct photo-etching method.

Figure 3 shows the etching depth as a function of SR photon fluence in the case of the native PTFE, RX-1600, and LMRX-1600 at 413 K. The etching rate of RX-1600 is higher than the one of native PTFE. Here, etching rate is defined as etching depth per unit irradiation time. Etching rate correlates with slope of Figure 3. Moreover, the

etching rate of LMRX-1600 is higher than the one of any other sample. The maximum etching rate of LMRX-1600 was 110 $\mu m \cdot min^{-1}$ when maximum accumulated current in the storage ring was 600 mA. (Here after, it is written as ring current.)

Since it has already been proved that the etching rate is hardly related to crystallinity and molecular weight (see Figure 4),[15] the higher etching rate of crosslinked PTFE could not be explained by the lower crystallinity and higher molecular weight of crosslinked PTFE. On the other hand, it is expected that the crosslinking density of LMRX-1600 is higher than that of RX-1600. Crosslinking density should be determined by the amount of generated radicals and the chain mobility of the starting material. Molecular motion of LM is much enhanced compared with that of native PTFE. Hence, it can be concluded that the etching rate of crosslinked PTFE depends on the amount of crosslinking point. Other experimental results that the etching rate of RX-3000 is higher than that of RX-1600 support our conclusion.[15]

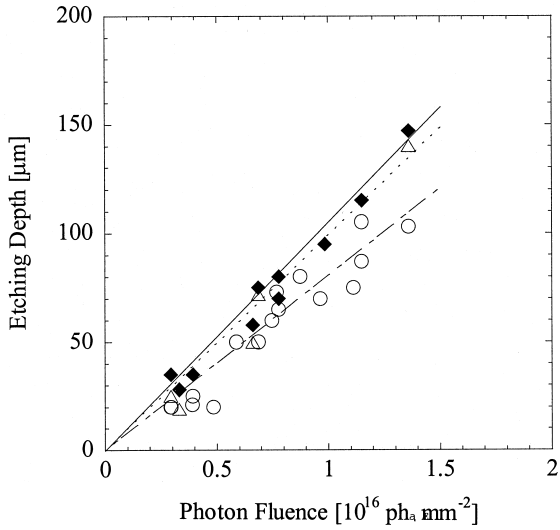

Figure 3. Relation between etching depth and SR photon fluence at 413 K in the case of native PTFE, RX-1600 and LMRX-1600; native PTFE: o, RX-1600: Δ, LMRX-1600: ♦.

The temperature dependence of the etching rate for native PTFE and RX-3000 is shown in Figure 5. As irradiation temperature is elevated, the etching rate becomes higher and the ratio of the etching rates of [RX-3000]/[native PTFE] is smaller. For example, the etching rate of RX-3000 is 1.5 times higher than that of native PTFE at 413 K, while the etching rate of RX-3000 is 2.1 times higher than that of native PTFE at 343 K. The

results shown in Figure 5 indicate that molecular motion of crosslinked PTFE would play an important role in SR etching process. When the network is formed in PTFE, the change of molecular conformation and mode of molecular motion takes place. While α-relaxation of non-crosslinked PTFE at 413 K comes from a mode of long molecular chains interpenetrating among crystallites, it is shown that α-relaxation for crosslinked PTFE (RX-3000 at 393 K) is related to the mode of long segments connecting crosslinking sites.[6,19] Moreover, the β-relaxation (native PTFE at 292K and 303K) disappeared by introducing crosslinking sites due to disordering of the helical conformation of the polymer chain in the crystals.[6,19]

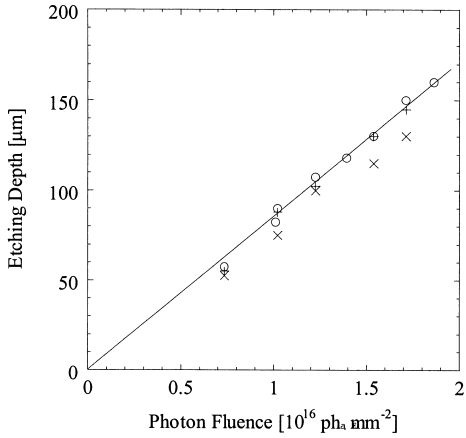

Figure 4. Relation between etching depth and SR fluence at 413 K in the case of native PTFE (o), LC (x) and LM (+)[15].

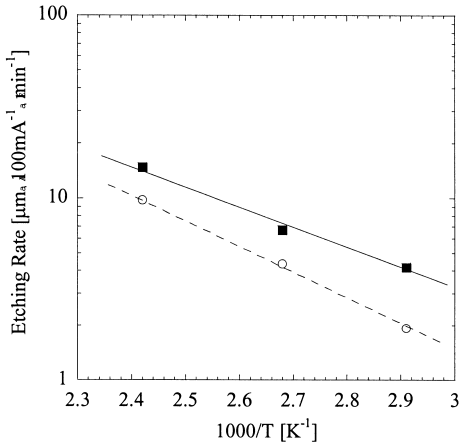

Figure 5. Temperature dependence of etching rate in the case of native PTFE (o) and RX-3000 (■).

Through crosslinking network formation, molecular motion of crosslinked PTFE should be enhanced above and even somewhat below the β-relaxation temperature. Oshima et al.[20,21] have already reported these facts by examining the decay curve of trapped radicals at elevating temperature. It may be reasonable to conclude that the enhanced molecular motion of crosslinked PTFE greatly accelerates decomposition and desorption.

Surface modification (for native PTFE)

In order to investigate SR induced reaction and desorption mechanism, we have analyzed the surface of SR-irradiated sample by FT-IR. The thickness of the SR-irradiated samples decrease with the irradiation time, since SR photo-etching proceeds in the surface region. The SR-irradiated samples with a thickness of 50 μm were prepared from native PTFE with a thickness of 500 μm for the measurements. SR irradiation was performed at 413 K and 473 K. Native PTFE with a thickness of 50 μm was also prepared. Figure 6 shows FT-IR spectra of these samples. It was found that some new bands appear in the spectra of SR-irradiated samples. The band at 1784 cm^{-1} is assigned to terminal double bond.[10,22] The bands at 1729 and 1716 cm^{-1} are attributed to internal double bonds.[10,23,24] The appearance of these bands indicates that SR-irradiation induces main chain scission and dissociation of C-F bond in the region which is penetrated by SR. Moreover, the weak absorption band at 1671 cm^{-1} can be observed. This band is due to -CF=C< which originates from defluorination around –CF<.[10,25] This result suggests that crosslinking reaction is also induced by SR-irradiation at 413 K. The peak at 1671 cm^{-1} can be observed in the spectra of crosslinked PTFE obtained by EB irradiation at 613 K.[10] In the previous paper, we have reported differential scanning calorimeter (DSC; DSC7 provided by Perkin Elmer) results suggesting the same fact that crosslinking reaction could be induced by SR-irradiation below the melting temperature of PTFE.[26]

Figure 7 shows spatial distribution of calculated SR dose rate at ring current of 300 mA corresponding to standard current of AURORA-2S. Details of the calculation are described in the Appendix. The dose rate in the surface region (depth from surface of 1 μm) is expected to be about 2 $MGy \cdot s^{-1}$, which is much higher than that of other beam (for example, typical dose rate of EB is a few $kGy \cdot s^{-1}$.). When PTFE sample absorbs such a high dose, a large amount of bond scission would be induced. Since produced fragments should be small enough, they would desorb from surface readily after the

decomposition. Moreover, dose rate around even inner region (depth from surface of a few tenth μm) is estimated to be 0.5 – 0.1 $MGy \cdot s^{-1}$, which is enough high compared with dose rate of other radiation source. The effect of high SR dose rate may explain the FT-IR results for SR induced crosslinking reaction. Although the recombination reaction among radicals proceeds due to the promoted mobility of molecular chain in the molten state, the free radicals formed in the solid state are restricted by the steric hindrance of molecular chain to react with the radicals formed in neighboring molecules. In spite of these facts known for EB induced crosslinking, our results show that crosslinking structure should be formed in the solid state. SR-irradiation of high dose rate should lead to generation of considerable amount of radicals and much shorter distance among generated radicals. Furthermore, the molecular motion in amorphous phase should be allowed over γ-relaxation temperature of 176 K. Therefore, radicals formed by SR-irradiation in amorphous phase would exceed structural restriction to react with other radicals and crosslinking network would be formed even in the solid state.

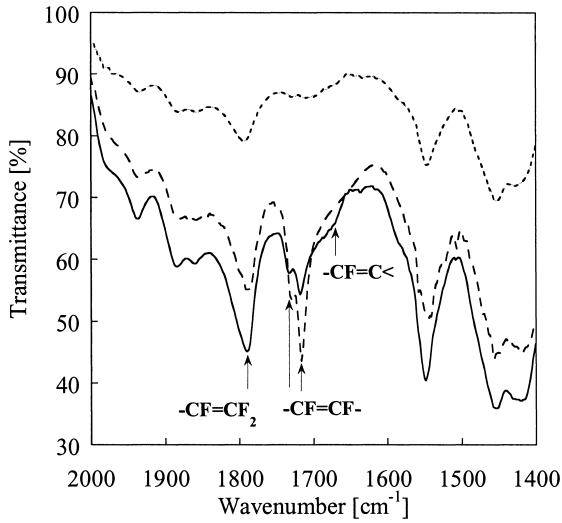

Figure 6. FT-IR spectra of SR-irradiated PTFE; ..... = native PTFE, ——— = SR-irradiated at 473 K, – – = SR-irradiated at 413 K.

SR induced network should be heterogeneous structure compared with already existing crosslinked PTFE by EB-irradiation in its molten state, because crosslinking reaction would be induced in just amorphous phase. Since large energy deposition could be achieved by high LET (linear energy transfer) beams such as heavy ions, they may be

able to induce the crosslinking reaction of PTFE in its solid state.

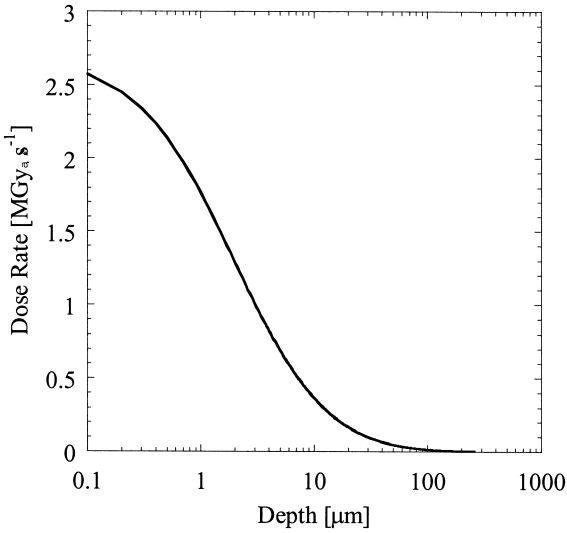

Figure 7. Spatial distribution of calculated SR dose rate at ring current of 300 mA.

Conclusion

Micromachining of crosslinked PTFE can be demonstrated by SR direct photo-etching method. The etching rate of crosslinked PTFE is higher than that of non-crosslinked PTFE and the ratio of the etching rate of crosslinked PTFE to that of non-crosslinked PTFE is higher at lower irradiation temperature. The etching rate depends on crosslinking density which is related to chain mobility and mode of molecular motion. SR modifies inner region, in which crosslinking reaction is induced much below the melting temperature due to SR high dose rate. These findings might be suitable for the development of microcomponents and other applications taking advantages of crosslinked PTFE, which is available not only in electronics or medical fields, but also in radiation fields.

Acknowledgements

The authors would like to acknowledge the staff of the Takasaki Radiation Chemistry Research Establishment (JAERI) for EB and γ-ray irradiation. The authors also would like to acknowledge Prof. Y. Hama and Research Associate T. Oka of Advanced Research Institute for Science and Engineering, Waseda University for FT-IR

measurements.

Appendix

The estimation of the spatial distribution of SR dose in PTFE sample is presented. Wheeler *et al.* described the calculation of monochromatic X-ray dose rate using Beer's Law in their report.[27] We have modified their procedure and applied it to the calculation for broad spectrum of SR.

For the calculations, the knowledge of attenuation length is needed. Attenuation length μ means the depth into the material measured along the surface normal where the intensity of x-rays $I(x)$ falls to e^{-1} of its value at the surface $I(0)$. Figure 8 shows X-ray attenuation length in PTFE.[28] The peak at 284 eV is due to C1s absorption and the peak at 697 eV is due to F1s absorption. Since F1s absorption edge is included in the energy range which we have used for the experiments, strong SR interaction with inner shell electron leading to high dose rate is expected.

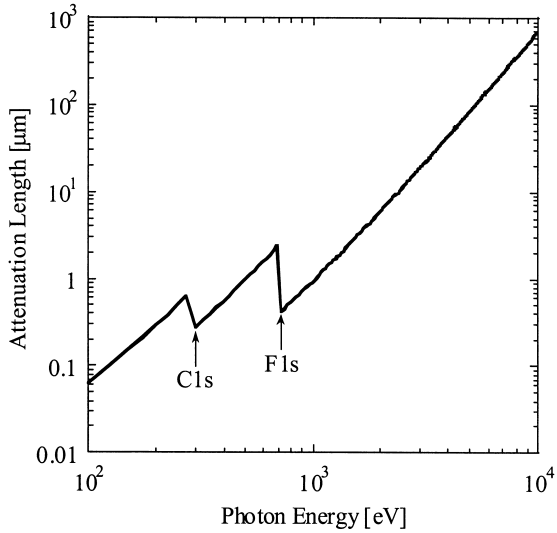

Figure 8. X-ray attenuation length in PTFE.

The intensity of the x-ray flux at depth x from the surface $I(x)$ is given by Beer's Law.

$$I(x) = I(0)\exp(-\mu^{-1}x) \quad (1)$$

Supposing the proportion from depth $x-\Delta x$ to $x+\Delta x$, the absorbed dose $D(x)$ by the proportion is

$$D(x) = h\nu \, (I(x-\Delta x) - I(x+\Delta x)) / 2\rho S\Delta x \quad (2)$$

where $h\nu$ is the photon energy, ρ is the density of PTFE and S is the SR exposed area. Since energy spectra of SR used in the experiment are broad (see Figure 1), equation (2) should be corrected as follows.

$$D(x) = \sum h\nu_i \, (I_i(x-\Delta x) - I_i(x+\Delta x)) \, / \, 2\rho S\Delta \, x \qquad (3)$$

$$= \sum h\nu_i \, I_i(0) \, (exp(-\mu_i^{-1}(x-\Delta x)) - exp(-\mu_i^{-1}(x+\Delta x))) \, / \, 2\rho S\Delta \, x \qquad (4)$$

The result of calculation at ring current of 300 mA is shown in Figure 7 using Δx = 0.01 μm, ρ = 2.2 g·cm^{-3}, Figure 1 as $I_i(0)/S$, and Figure 8 as μ_i.

[1] H. Mark, N. Bikales, C. Overberger, G. Menges, in: *"Encyclopedia of Polymer Science and Engineering"*, 2nd ed., J. Wiley & Sons, New York, 1964, Vol. 16, p. 577.
[2] M. Dole, in: "*The Radiation Chemistry of Macromolecules"*, Academic Press, New York, 1973, Vol. II, Chap. 9.
[3] Y. Tabata, *Proc. of Taniguchi Conf. "Solid state reaction in radiation chemistry."*, Sapporo, Japan, **1992**, 118.
[4] J. Sun, Y. Zhang, X. Zhong, X. Zhu, *Radiat. Phys. Chem.* **1994**, *44*, 655.
[5] A. Oshima, Y. Tabata, H. Kudoh, T. Seguchi, *Radiat. Phys. Chem.* **1995**, *45*, 269.
[6] Y. Tabata, A. Oshima, K. Takashika, T. Seguchi, *Radiat. Phys. Chem.* **1996**, *48*, 563.
[7] Y. Tabata, A. Oshima, *Macromol. Symp.* **1999**, *143*, 337.
[8] A. Oshima, S. Ikeda, T. Seguchi, Y. Tabata, *Radiat. Phys. Chem.* **1997**, *49*, 279.
[9] E. Katoh, H. Sugisawa, A. Oshima, Y. Tabata, T. Seguchi, T. Yamazaki, *Radiat. Phys. Chem.* **1999**, *54*, 165.
[10] A. Oshima, S. Ikeda, E. Katoh, Y. Tabata, *Radiat. Phys. Chem.* **2001**, *62*, 39.
[11] S. Wada, H. Tashiro, K. Toyota, H. Niino, A. Yabe, *Appl. Phys. Lett.* **1993**, *63*, 211.
[12] H. Kumagai, K. Midorikawa, K. Toyoda, S. Nakamura, T. Okamoto, M. Obara, *Appl. Phys. Lett.* **1994**, *65*, 1850.
[13] Y. Zhang, T. Katoh, M. Washio, M. Yamada, S. Hamada, *Appl. Phys. Lett.* **1995**, *67*, 872.
[14] T. Katoh, N. Nishi, M. Fukagawa, H. Ueno, S. Sugiyama, *Sensor and Actuators* **2001**, *A89*, 10.
[15] D. Yamaguchi, T. Katoh, S. Ikeda, M. Hirose, Y. Aoki, M. Iida, Y. Tabata, M. Washio, *Proc. of RadTech Japan 2000 Symp.* Yokohama, Japan, **2000**, 170.
[16] A.L. Ryland, *J. Chem. Educ.* **1958**, *35*, 80.
[17] T. Suwa, M. Takehisa, S. Machi, *J. Appl. Polym.* **1973**, *17*, 3253.
[18] Y. Zhang, T. Hori, *Synchrotron Radiat. News* **2000**, *13*, 32.
[19] A. Oshima, S. Ikeda, T. Seguchi, Y. Tabata, *Radiat. Phys. Chem.* **1997**, *49*, 581.
[20] A. Oshima, T. Seguchi, Y. Tabata, *Radiat. Phys. Chem.* **1997**, *50*, 601.
[21] A. Oshima, T. Seguchi, Y. Tabata, *Polym. Int.* **1999**, *48*, 996.
[22] M. I. Bro, C. A. Sperati, *J. Polym. Sci.* **1959**, *38*, 289.
[23] K. Lunkwitz, A. Ferse, P. Dietrich, G. Engler, U. Groß, D. Prescher, J. Schulze, *Plaste und Kautschuk* **1979**, *26*, 318.
[24] K. Lunkwitz, U. Groß, V. Glöckner, *Acta Polymerica* **1985**, *36*, 431.
[25] U. Lappan, U. Geißler, K. Lunkwitz, *Radiat. Phys. Chem.* **2000**, *56*, 317.
[26] T. Katoh, D. Yamaguchi, Y. Sato, S. Ikeda, Y. Aoki, M. Washio, Y. Tabata, *Appl. Surf. Sci.* in press.
[27] D. R. Wheeler, S. V. Pepper, *J. Vac. Sci. Technol.* **1990**, *A8*, 4046.
[28] B. L. Henke, E. M. Gullikson, J. C. Davis, *Atomic Data and Nuclear Data Tables*. **1993**, *54 (no.2)*, 181.